3rd International Conference "From Scientific Computing to Computational Engineering
3rd IC-SCCE
Athens, 9-12 July, 2008

PREDICTION OF THE BLOOD FLOW FIELD IN THE CAROTID-JUGULAR SHUNT USING FLOW AND PRESSURE MEASUREMENTS AND COMPUTATIONAL FLUID MECHANICS

T.A. Manos[1], D.P. Sokolis[2], A.T. Giagini[2], C.A. Dimitriou[2], C.H. Davos[3], M.G. Peroulis[4], P.E. Karayannacos[2], S. Tsangaris [1]

[1]Laboratory of Biofluid-Mechanics and Biomedical Engineering,
National Technical University of Athens, Athens, Greece
[2]Center of Experimental Surgery, Foundation of Biomedical Research, Academy of Athens, Athens, Greece
[3]Center of Clinical Research, Foundation of Biomedical Research, Academy of
Athens, Athens, Greece
[4]Vascular Unit, 3rd Department of Surgery, University of Athens School of Medicine, Attikon University
Hospital, Athens, Greece

Keywords: CFD, in vivo, 3D, Angiography, Intimal hyperplasia.

Abstract. *One of the chief factors, incriminated for the formation of intimal hyperplasia at the venous side of an arteriovenous anastomosis (AVA), is the disturbed hemodynamic condition in that region. Owing to the difficulty of properly measuring the local flow field near AVA, numerical computation has been extensively used for its assessment.*

The purpose of this study was to examine the flow field in AVA with computational fluid dynamics (CFD). AVAs were created in pigs between the common carotid artery and the internal jugular vein using ePTFE grafts. Input data to the computational model was obtained in vivo one month later, and adjacent vessels were excised and submitted to histological examination. The 3D geometry of the anastomosis was determined using biplane angiography. Ultrasound measurements of the flow rates were performed with perivascular flow probes. Pressures were recorded using intravascular catheters. This data was used as boundary conditions in the commercial code FLUENT® for calculation of the flow field.

Our numerical findings are suggestive of strong Dean vortices towards both vein flow exits, verified by colour Doppler. The high wall shear stresses that accompany these vortices are related to areas of intimal hyperplasia, as evidenced in preliminary histological studies of the venous vessel wall.

1. INTRODUCTION

The arteriovenous shunt (AVS) is the surgical connection of an artery to a vein through a graft, which is created in hemodialysis patients as an access site. Polytetrafluroethylene (PTFE) is often used as a synthetic graft material for that purpose. Unfortunately, more than half of the AV grafts are occluded and fail due to the formation of intimal hyperplasia at the venous side of AVS, so that surgical reconstruction may be necessary within three years [1].

Various factors have been proposed to predispose to graft failure the most important of those being mechanical injury of the host vein, mismatched compliance between graft and vein and the disturbance of haemodynamic conditions in the region of anastomosis [2][3].

This paper presents a combined in vivo & numerical study, with the purpose of examining the haemodynamics associated with intimal thickening in AVS. A subject-specific geometry was employed together with boundary conditions obtained from in vivo flow and pressure measurements. The numerical results were correlated with the corresponding color Doppler ultrasound and histomorphological findings. Few are the studies, where this kind of data association has been carried out so far.

2. MATERIALS AND METHODS

2.1. Animals

A healthy male Landrace pig weighing 65 kg underwent surgical exposure of the right common carotid artery and ipsilateral internal jugular vein, and creation of an AVS via an expanded (e-PTFE) graft, according to the model by Rotmans et al[4]. The animal was sacrificed 1 month postoperatively. Animal housing and handling complied with the guiding principles of the American Physiological Society and the Greek Presidential Decree 160/1991, issued after the European Union Directive 609/1986. The experimental protocol was approved by the ethics committee of the Foundation of Biomedical Research of the Academy of Athens.

2.2. Surgical procedures

Starting 6 days preoperatively, the animal received 100 mg/day acetylsalicylic acid (Salospir; Unipharm), 75 mg/day clopidogrel (Plavix; Sanofi Aventis), and 25 mg/day digoxin (Digoxin; Sandoz) until termination, with the latter stopped on the 8th day postoperatively. On the day of surgery, animals were fasted overnight and sedated intramuscularly with 10 mg/kg ketamine (Imalgen; Merial), 4 mg/kg azaperone (Suicalm; Jansen-Cilag), and 0.05 mg/kg atropine (Atropine; Demo). Anaesthesia was induced, 15 min later, with intravenous administration of 0.9 mg/kg propofol (Diprivan 1% w/v; AstraZeneca). During induction of anesthesia, blood pressure was monitored non-invasively every 3 min and as required with a pressure sphygmomanometer placed at the right front limb of the animal. External ECG leads were placed for monitoring heart rate. Animals were connected to an anesthetic machine (MDS Matrx; Orchard Park, NY, USA) and a volume control respirator (Model 2000; Hallowell EMC, Pittsfield, MA, USA). Sevoflurane (Sevorane; Abbott) 3-5 % (vaporizer setting) in oxygen was administered for the maintenance of anaesthesia.

Under sterile conditions, a midline cervical incision was made, and the right common carotid artery and ipsilateral internal jugular vein were exposed. Papaverine (5 mg/ml) was instilled locally to avoid vasospasm. Heparin (iv, 200 IU/kg) was given before manipulation of the vessels. The artery was clamped using atraumatic clamps and an 8-mm arteriotomy was performed. An end-to-side anastomosis was created at a 45º angle using a continuous 8-0 polypropelene suture. Reinforced, thin-walled, ringed, e-PTFE grafts of 6-mm diameter and 10-cm length were used (Advanta VS; Atrium Medical Corp, Hudson, NH, USA). The venous anastomosis was created similarly.

2.3. Euthanasia and tissue preparation

Before the animal was sacrificed, it was premedicated and anesthetized as above. The midline neck incision was reopened and the carotid artery and jugular vein carefully exposed once more. Flow and pressure measurements were conducted as described below. The animal was sacrificed with a bolus dose of pentobarbital sodium and the anastomosed and control tissues were cautiously excised to avoid damage to their walls. The contralateral internal jugular vein served as control. For both cases, the adherent connective tissue was carefully trimmed and the specimens were prepared for the histomorphometrical study.

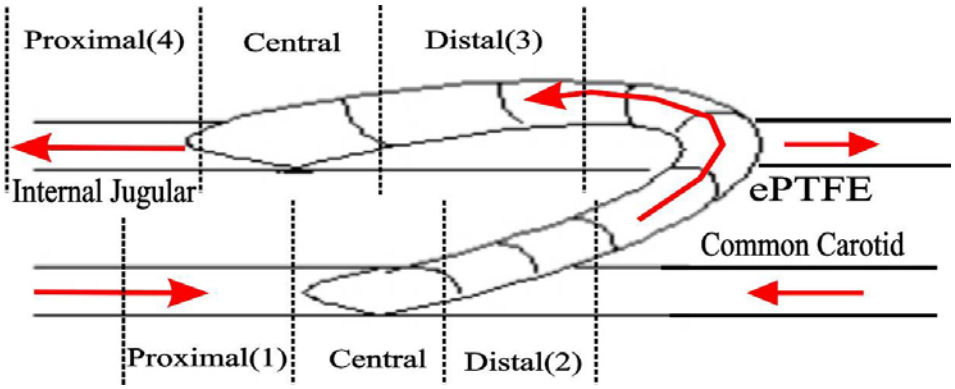

Figure 1. Schematic representation of AVS via an ePTFE graft between the common carotid artery and internal jugular vein, and the numbering of specimens

2.4. Hemodynamic measurements

All necessary measurements used for the CFD model were obtained 1 month after graft implantation. The flow field at the anastomosis was inspected preoperatively with the cardiovascular colour flow Doppler ultrasound system (Vivid 7, GE Medical Systems, Milwaukee, WI, USA), using it's linear array vascular probe (size 12L) at colour and pulse wave Doppler modes. Blood flows at the proximal (position 1) and distal (position 2) artery, and at the proximal (position 3) and distal (position 4) vein were measured using the perivascular ultrasonic flow probes (TA 420; Transonic Systems, Ithaca, NY, USA) of appropriate size, Figure 1. Pressure at the proximal vein was determined with a 5F catheter-tipped pressure transducer (SPC-450; Millar Instruments, Houston, TX, USA), Figure 2. Blood flow was recorded first at the vein and then at the artery, because of shortage in appropriate probe sizes. Pressure was recorded simultaneously with the flows, only in the artery. Recordings were performed under a hemodynamicaly stable condition; presumably when pressures and flows did not exhibit temporal variations for about 5 min. This practically meant waiting for 10 min if no vasospasm was apparent or 30 min otherwise. All data signals were simultaneously recorded by a digital acquisition system

(Sonometrics System; Sonometrics Co, Ontario, Canada) at 60-sec data epochs with a sampling rate in excess of 300 Hz, during which the respirator was turned off to avoid respiration-induced noise. Afterwards, the flow field at the anastomosis was inspected once more with the cardiovascular ultrasound system; with the image acquisition made intraoperatively by use of the linear array cardiac intraoperative probe (size i13L).

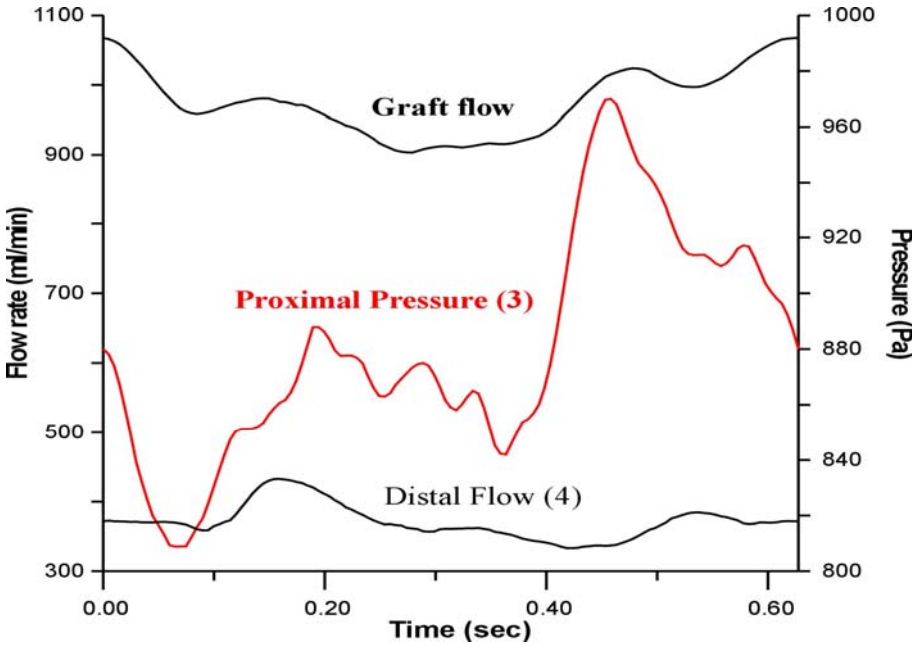

Figure 2. Recordings of flow rate at the graft inlet (black line) of pressure (red line) at the distal outlet (position 3) and of flow rate (black line) at the proximal outlet (position 4).

2.5. Biplane angiography

Subsequent to exposure of the carotid artery and jugular vein, and to hemodynamic measurements, biplane angiography was carried out using a C-arm mobile diagnostic X-ray image acquisition and viewing system (BV Libra; Philips Medical Systems, P.M.G Surgery, The Netherlands). A catheter was inserted into the graft. The C-arm was tested at various angles to avoid adjustments during image acquisition. Contrast media was then administered and digital subtraction angiography was performed at three selected angles, allowing unambiguous identification of the venous anastomosis. The monitor output was recorded on DVD, Figure 3 (left).

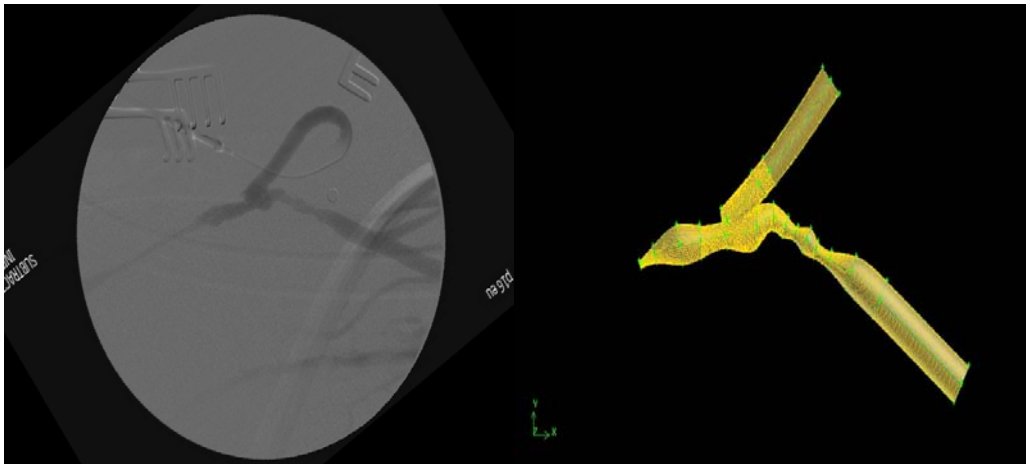

Figure 3. Angiography of graft – jugular vein anastomosis (left) and 3D mesh of the anastomosis generated by GAMBIT (right).

2.6. Histomorphometrical studies

Following animal euthanasia, tissue from the region of venous anastomosis was removed and cut into three parts of equal length: the central, proximal and distal to the anastomosis tissue segments, Figure 1.

Specimens from the three regions were fixed with 10% buffered formalin over 24 hours, dehydrated in graded ethanol and xylol, and embedded in paraffin wax. Serial 5-μm thick sections were cut on a microtome (Leica RM 2125; Leica, Nussloch, Germany) and treated with picro-Sirius red for collagen matrix and orcein for elastin fiber staining.

Images were taken by a digital camera (Altra 20; Soft Imaging System, Muenster, Germany) fitted to a light microscope (Olympus CX31; Olympus, Tokyo, Japan) and processed using a commercial image-analysis software (Image-Pro Plus v.6.0; Media Cybernetics Inc, Silver Spring, MD, USA). The thickness of tunica intima, media and adventitia, and the entire vessel wall was measured. Elastin and collagen area densities for the three layers were also measured after the micrographs were segmented using the software. These were calculated with respect to the total area of that layer in the region of interest. The area densities for the entire vessel were calculated using the respective ones for the three layers, and their thicknesses. Values for each specimen were averages from three sections.

2.7. Postoperative data editing and analysis

The data stored in the Sonometrics console was used as boundary conditions after careful editing. The flow rates at the proximal and distal carotid artery were added to obtain the graft inlet flow. The same was done for the proximal and distal jugular vein. Pressure and flow signals were delineated according to cardiac cycle. Synchronization of the two recordings was performed by a reference signal, i.e. the flow through the graft. A characteristic cardiac pulse was selected and extracted in ascii format for further processing. Data analysis was carried out with the Sonosoft software (Sonometrics Co).

Next to importing the pulse data in Excel (Microsoft Office Excel 2003), all signals were modified to remove the linear drift caused by the temporal variation of hemodynamics at the anastomosis. The flows were also adjusted to account for the relative difference, because of the probe accuracy, Figure 2.

From the modified signals, we selected the graft and distal vein flow as well as the proximal vein pressure for processing in MATLAB, because these were used as boundary conditions for our models. This data was first re-sampled based on a common time vector, and then smoothed and curve-fitted using a Fourier fit of eighth degree.

2.8. Reconstruction of geometry and mesh development

The three angles, at which the monitor output was recorded, were studied and appropriate images were selected for geometrical reconstruction. Using the Info Cliper software (Canopus Co, Ltd. UK), images of interest were captured in bmp format. In the case studied, the venous anastomosis was planar and its plane was perpendicular to the surgical table, simplifying the reconstruction. There was no need for a reconstruction algorithm; only one image at an axis vertical to the plane of anastomosis was required, Figure 3.

The selected image was rotated, filtered and segmented using the Image-Pro Plus software. Then, the vessel centreline and boundaries were traced manually by point selection with Paint Shop Pro 5 (Copyright 1991-1998, Jasc Software, Inc. MN, USA). This modified image was processed by a developed MATLAB code, which extracted the coordinates of the points selected. The point cloud was then imported into GAMBIT (v. 2.3.16, Fluent Inc., Lebanon, NH, USA). The three dimensional geometry was reconstructed assuming circular cross-sections of varying diameter for the graft and vessel. The model was first cut in the middle, taking into account the planar symmetry, which aided to decrease the total number of elements. Afterwards, the geometry was split into four regions: the junction, proximal venous segment, distal venous segment and graft inlet. In the junction, an unstructured grid was used that consisted of wedge, tetrahedron and pyramidal elements, while for the other three volumes a structured grid with hexahedron elements was used, Figure 3. The total element count was 173177.

2.9. Numerical simulation

The mesh generated was exported in the appropriate format to the finite volume solver Fluent (version 6.2.16, Fluent Inc, Lebanon, NH, USA). Blood was approximated as a Newtonian fluid with a viscosity of 3.6×10^{-3} Pa·s and a density of 1000 kg/m^3. Flow was assumed to be laminar and steady. For boundary conditions, the mean values of pulse pressure and flows were considered. A plug velocity profile of 0.47 m/s was assumed or the graft. For the proximal venous segment (position 4), an exit plug velocity profile was also assumed with a constant velocity of 4.57 m/s. At the other venous exit (position 3), a pressure outlet condition was used with constant pressure of 6.6 mmHg (880 Pa). The Navier-Stokes equations were solved by using a

segregated solver with an implicit formulation, while for the pressure discretization a PRESTO! scheme and for the momentum a first order upwind scheme were used. The pressure-velocity coupling method of choice was the PISO algorithm. The convergence criteria, defining the end of the iterative process, were continuity and momentum residuals of 0.0001. In a future study the unsteady case will be examined, where the pulse waveforms will be used as inputs.

3. RESULTS

3.1. Numerical simulation results

The flow patterns observed were complex and highly three dimensional, due to the complex geometry of AVS one month after its creation. In Figure 4, the contours of velocity magnitude are shown at the symmetry plane of the model geometry, while in Figure 5 the velocity vectors at the same plane are shown but zoomed in on the junction region of anastomosis. From these figures, the following may be deduced: Flow enters the graft as a plug velocity profile, but as approaches the host vessel it becomes fully developed. Part of the flow, before entering the junction region, collides with the wall of the bulge that is present near the toe section and a recirculation zone evolves at that point. In contrast, the main part of flow strikes the floor of the host vessel and separates into two streams of opposing directions. A stagnation point is formed at the point of division.

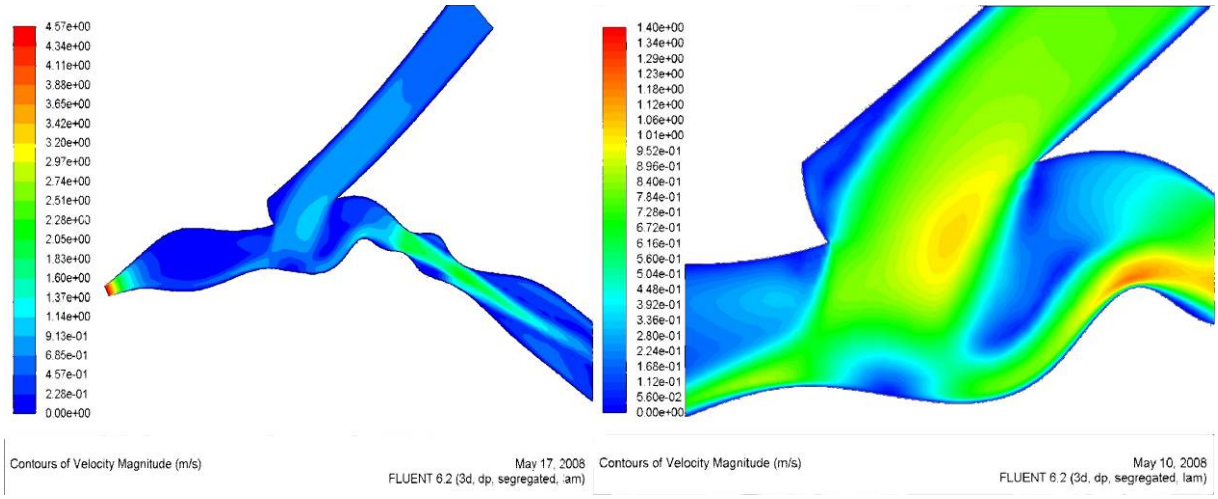

Figure 4. Velocity magnitude at the symmetry plane (left) and zoom in on the junction region (right).

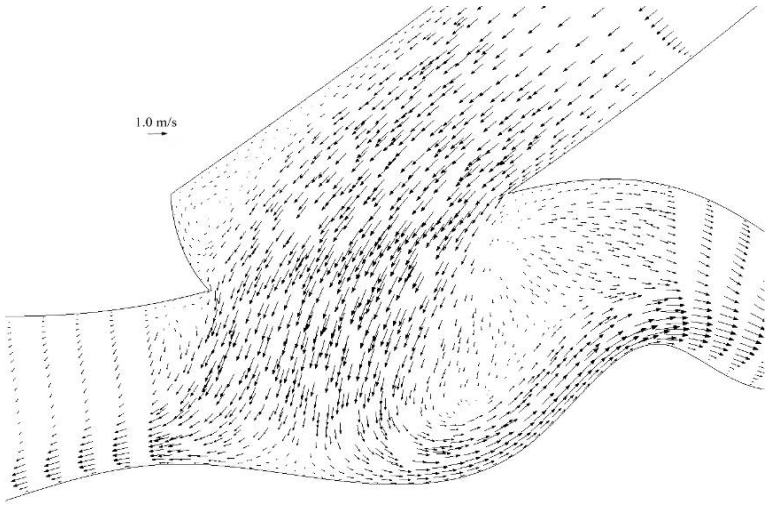

Figure 5. Velocity vectors at the symmetry plane of the junction region.

Following that part of the stream, heading towards the proximal segment exit (position 4), we notice that as it turns on the flow dividing wall, it sets up a Dean flow pattern in which flow on the lateral walls moves upwards towards the toe, Figure 7 (left). These counter rotating vortices have their center near the toe wall at the start, but as they move downstream their center approaches the vessel axis. At the proximal segment exit (position 4),

there is a vessel contraction, where the vessel lumen has it smallest cross sectional area. Maximum flow velocities of 4.5 m/s are noted there.

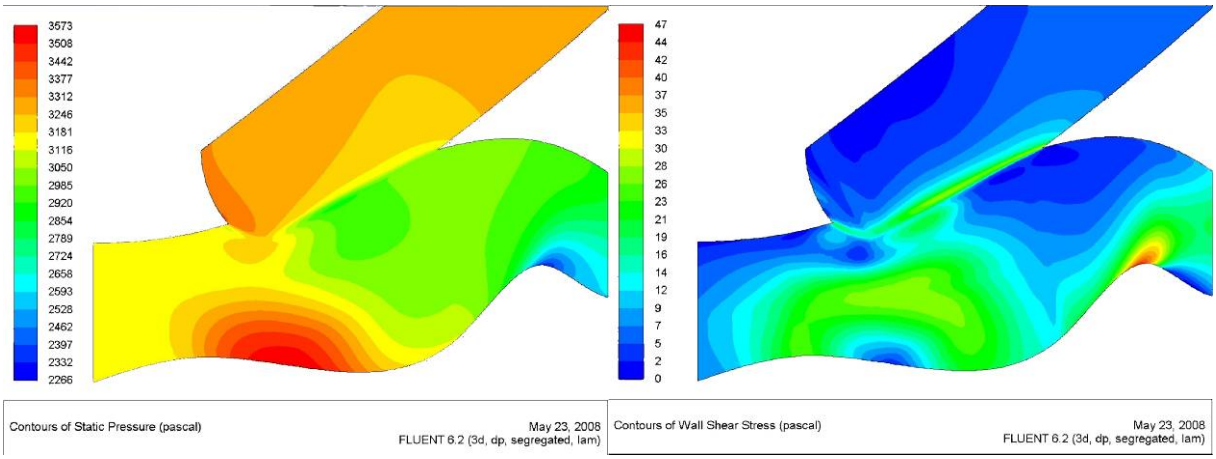

Figure 6. Contours of wall static pressure (left) and wall shear stresses (right) at the junction region.

The other part of inlet flow, which divides at the stagnation point region, moves towards the distal exit (position 3). This stream also forms Dean vortices, accompanying it until it reaches the exits, but with a diminishing effect. This venous segment exhibits two stenotic regions lying close to each other. The first stenosis creates a strong jet stream that passes through the expansion zone between the two stenoses and enters the final one. High velocities of about 2 m/s are detected at these stenotic areas. Finally, the jet stream and counter rotating vortices slowly attenuate downstream, as the flow develops close to the exit.

Wall shear stress contours for the junction region are displayed in Figure 6 (left). The mean value for shear stresses of the model is about 6.0 Pa, consistent with the value reported by Harugushi et al [3]. The maximum value of 815 Pa was found at the stenosis of the proximal exit (position 4). Other regions of high wall shear stresses were the first, i.e. 100 Pa, and second stenosis, i.e. 70 Pa, of the distal part, the floor of distal venous segment opposite to the heel region, i.e. 45 Pa, and finally the region around the stagnation point on the lateral walls of the host vessel, i.e. 27 Pa.

The wall pressure distribution at the junction region is displayed in Figure 6 (right). Pressure is a prominent factor, which contributes to vessel wall remodeling [5]. The highest values are found at the stagnation point, about 3570 Pa, while the regions of lowest pressure are registered opposite to the heel region, i.e. 2350 Pa, as a consequence of the high velocities that exist there. The model's minimum value of -12000 Pa is observed at the proximal exit (position 4), because of the severe stenosis. The maximum values are noted at the inlet and proximal segment region, about 3000 Pa. Lower values exist at the distal segment, because of the flow turn and two distal stenoses. As flow enters the first stenosis, pressure is 2700 Pa, dropping to 500 Pa at the stenosis. Pressure then increases to 1000 Pa at the expansion region between the two stenoses, drops once again to 200 Pa at the second stenosis, and recovers a value of 800 Pa at the expansion zone that follows.

3.2. Histomorphometrical results

Table 1 shows the histomorphometrical results of our study. Of the three vessel layers examined, the changes found in tunica intima and media were most significant, the reason being that these layers were affected to a greater extent by the disturbed flow, owing to their close proximity to it.

After a close inspection of the table, we deduce that there is an increase in thickness of all layers at all positions of the anastomosis compared to control, except for a single case. The adventitia exhibits small variations, while for the other two layers there is profound increase in thickness, which attests to the fact that intimal hyperplasia is present [7],[8]. For tunica intima, a ten-fold thickness increase is noted at the distal segment and a three-fold increase at the proximal one. Thickness variation is much smaller at the central segment. The opposite is true for tunica media, where the greatest change is found at the central region.

Concerning the elastin area density, there is a decrease in the anastomosed compared to control tissue in all cases. This is in agreement with the literature, according to which areas of high velocities and wall shear stresses are correlated with a decrease in elastin content [7],[9]. At some instances, the variation is slight while at others elastin content is less than half, compared to control values, as in the proximal segment. Collagen results are less definite. In half of the cases there is collagen content increase in anastomosed tissue, while for the other half the opposite is true.

		Intima	Media	Adventitia	Total
Vessel wall thickness (μm)					
Anastomosis	Proximal	40,1315 ± 2,0236	381,7441 ± 41,2858	339,1003 ± 31,7479	760,9759 ± 41,1321
	Central	19,4397 ± 0,7070	331,7690 ± 9,6318	104,1622 ± 1,9445	455,309 ±9,7721
	Distal	307,7802 ± 85,7938	197,0018 ± 18,9499	396,8828 ± 12,5439	901,6648 ± 81,7383
Control	Proximal	14,2327 ± 0,9324	132,7916 ± 16,8127	177,5676 ± 14,7165	324,5919 ± 26,9989
	Central	15,0854 ± 0,8472	59,0266 ± 2,6998	130,7260 ± 11,0051	204,8380 ± 10,8410
	Distal	28,8508 ± 2,3296	139,4866 ± 10,9493	264,3458 ± 18,4450	432,6831 ± 23,2326
Collagen area density (%)					
Anastomosis	Proximal	17,9613 ± 1,2676	23,5770 ± 0,9593	21,2556 ± 1,7126	22,24640083
	Central	16,9068 ± 1,0184	12,9602 ± 0,7195	17,7192 ± 1,0182	14,21726019
	Distal	13,5686 ± 4,3945	13,3602 ± 1,9568	19,34411 ± 2,3969	16,06525442
Control	Proximal	25,5296 ± 1,1020	11,7837 ± 1,6340	18,3111 ± 0,9023	15,95723613
	Central	8,2167 ± 0,8709	12,4153 ± 0,9917	16,6824 ± 0,5091	14,82932159
	Distal	21,5265 ± 1,5814	14,7018 ± 0,5006	21,2221 ± 2,2554	19,12388061
Elastin area density (%)					
Anastomosis	Proximal	8,0879 ± 1,0987	6,9593 ± 2,2687	8,4316 ± 0,4566	7,674893993
	Central	10,3121 ± 0,8738	4,7941 ± 0,3643	8,0287 ± 0,4811	5,7695495
	Distal	4,2504 ± 0,7265	6,1430 ± 1,2917	9,9586 ± 0,4769	7,176467432
Control	Proximal	15,4699 ± 0,5337	9,3120 ± 0,8563	11,8819 ± 1,3978	10,98787213
	Central	13,8782 ± 0,7411	5,9990 ± 0,7491	14,7454 ± 0,9402	12,16115141
	Distal	11,9494 ± 0,3933	13,5749 ± 0,7455	15,5610 ± 0,9119	14,66464912

Table 1. Results from histomorphometrical analysis for the anastomosed and control tissue.

4. Discussion

The flow in the anastomosis junction was highly complex and exhibited many features not reported in previous studies. The reason for this, is that the geometry was subject-specific, based on the angiography taken from a porcine AVS one month post-implantation. This meant that the vessel studied had remodeled and intimal hyperplasia had developed, distorting the initial geometry.

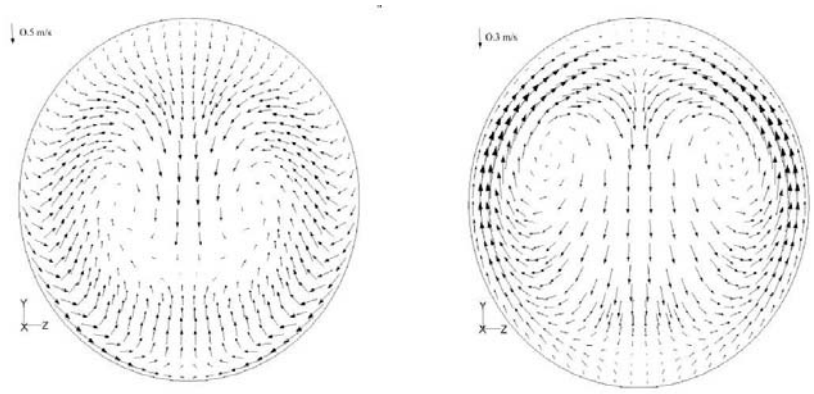

Figure 7. Velocity vector plots showing Dean vortices at cross-sections of the junction region. Proximal segment (left); distal segment (right).

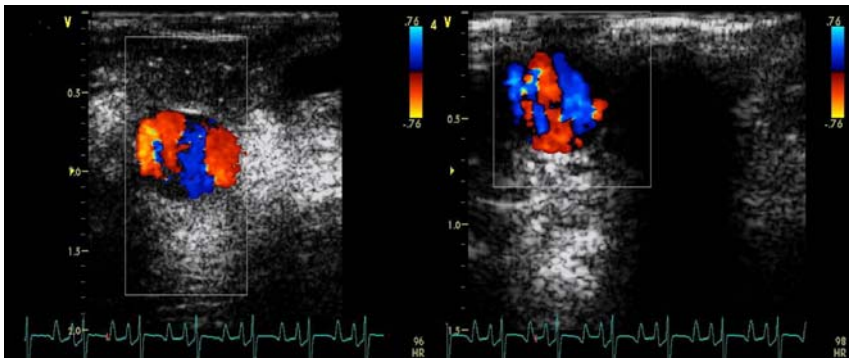

Figure 8. Dean vortices at cross-sections obtained intraoperatively by color Doppler ultrasound. Proximal segment (left); distal segment (right).

The patient-specific geometry examined had many irregularities. These were: a) the bulge at the toe area, b) the stenosis at the proximal segment exit, and c) the stenoses at the distal segment. The bulge might have been caused by the way the graft had been sutured and by intimal hyperplasia, owing to the resulting disturbed flow. For the other two vessel formations, intimal hyperplasia must have been again the reason. It is known fact that at the proximal segment of AV grafts there is an extended toe and floor region, where hyperplasia is noted [2][3].

The reasons incriminated for its development are high wall shear stresses and high wall shear stress gradients [3]. Our numerical results confirmed those findings at the far proximal segment, but not at the toe region. In contrast to the literature the distal segment did also exhibit high wall shear stresses. We believe that this may be reminiscent of the fact that after constriction of the proximal segment, the flow in the distal one increased, eliciting high wall shear stresses.

Our histomorphometrical results suggested that the distal segment close to the heel was affected the most. At this region there is a ten-fold increase in thickness of tunica intima, validating the existence of intimal hyperplasia. The elastin content of that region also varied significantly, as values were less than half the ones found for control. Both alterations in vessel structure are correlated with high wall shear stresses in the literature [3], [4], [8], [10], [11]. The numerical simulation performed in this study showed that the highest wall shear stresses of the junction region were found at the host vessel floor opposite to the heel, at the distal segment. This observation may be related to the increased wall thickness and decreased elastin content.

The most interesting flow features noted were the Dean vortices that developed in both segments. These counter rotating vortices have been also noted in other numerical studies [1],[6] for the proximal segment, although the geometry and flow conditions were different. The same is not true for the Dean flow noticed at the distal segment one. The existence of both vortices was validated by the color Doppler ultrasound (Figure 8).

There are limitations with the present numerical study. The vessel wall distensibility was ignored and the fluid was assumed to be Newtonian, which is a good approximation for large vessels. Furthermore, the geometry portrayed the remodeled vessel, just prior to the loss of patency; so that we examined the result of disturbed flow. It would have been interesting to also study the initial un-remodeled geometry. Finally, the flow was considered as steady, although it was pulsating. In a subsequent investigation, the known pressure and flow waveforms will be used as boundary conditions for an unsteady numerical simulation.

ACKNOWLEDGEMENTS

This paper is part of the 03ED 262 research project, implemented within the framework of the "Reinforcement of Human Research Manpower" (PENED) and co-financed by National and Community Funds (25% from Greek Ministry of Development – General Secretariat of Research and Technology and 75% from E.U. – European Social Fund).

REFERENCES

[1] Loth, F., Fisher, P.F., Arslan, N., Bertram, C.D., Lee, S.E., Royston, T.J., Shaalan, W.E. and Bassiouny, H.S. (2003), "Transitional Flow at the Venous Anastomosis of an Arteriovenous Graft: Potential Activation of the ERK1/2 Mechanotransduction Pathway", J. Biomech. Eng., Vol. 125, pp. 49-61.

[2] Loth, F., Fischer, P.F. and Bassiouny, H.S. (2008), "Blood Flow in End-to-Side Anastomoses", Annual Review of Fluid Mechanics, Vol. 40, pp 367-393.

[3] Haruguchi, H. and Teraoka, S. (2003), "Intimal hyperplasia and hemodynamic factors in arterial bypass and arteriovenous grafts: a review", J. Artif. Organs., Vol. 6, pp.227-235.

[4] Rotmans, J.I., Velema, E., Verhagen, H.J.M., Blankensteijn, J.D., Kastelein, J.J.P., de Kleijn, D.P.V., Yo, M., Pasterkamp, G. and Stroes, E. S.G. (2003), "Rapid, Arteriovenous Graft Failure Due to Intimal Hyperplasia: A Porcine, Bilateral, Carotid Arteriovenous Graft Model", Journal of Surgical Research, Vol. 113, pp. 161-171.

[5] Hayashi, K., Mori, K. and Miyazaki, H. (2003), "Biomechanical response of femoral vein to chronic elevation of blood pressure in rabbits", Am. J. Physiol. Heart Circ. Physiol., Vol. 284, pp. H511-H512.

[6] Chen, J., Lu, X.Y. and Wang, W. (2006), "Non-Newtonian effects of blood flow on hemodynamics in distal vascular graft anastomoses", J. Biomech., Vol. 39, pp. 1983-1995.

[7] Rotmans, J.I., Velema, E., Verhagen, H.J.M., Blankenstejin, J.D., Kleijn, D.R.V., Pasetrkamp, G. and Stroes, E.S.G. (2004), "Matrix metalloproteinase inhibition reduces intima hyperplasia in a procine arteriovenous-graft model", J. Vasc Surg., Vol. 39, pp. 432-439.

[8] Tran-Son-Tay, R., Hwang, M., Berceli, S.A., Ozaki, C.K. and Garbey, M. (2007), "A model of vein graft intimal hyperplasia", Conf Proc IEEE Eng Med Biol Soc., pp. 5807-5810.

[9] Misra, S., Woodrum, D.A., Homburger, J., Elkouri, S., Mandrekar, J.N., Barocas, V., Glockner, J.F., Rajan, D.K. and Mukhopadhyay, D. (2006), "Assessment of Wall Shear Stress Changes in Arteries and Veins of Arteriovenous Polytetrafluoroethylene Grafts Using Magnetic Resonance Imaging", Cardiovasc Intervent Radiol. Vol. 29, pp. 624-629.

[10] Wentzel, J.J., Janssen, E., Vos, J., Schuurbiers, J.C., Krams, R., Serruys, P.W., de Feyter, P.J. and Slager, C.J. (2003), "Extension of increased atherosclerotic wall thickness into high shear stress regions is associated with loss of compensatory remodeling" Circulation, Vol. 108, pp. 17-23.

[11] Hofstra, L., Bergmans., D.C., Leunissen, K.M., Hoeks, A.P., Kitslaar, P.J., Daemen, M.J. and Tordoir, J.H. (1995), "Anastomotic intimal hyperplasia in prosthetic arteriovenous fistulas for hemodialysis is associated with initial high flow velocity and not with mismatch in elastic properties", J Am Soc Nephrol, Vol. 6, pp. 1625-1633.